PHYSICAL REVIEW B VOLUME 42, NUMBER 9 15 SEPTEMBER 1990-II

EPR identification of the single-acceptor state of interstitial carbon in silicon

L. W. Song* and G. D. Watkins

Department of Physics and Sherman Fairchild Center for Solid State Studies, Lehigh University, Bethlehem, Pennsylvania 18015

(Received 23 January 1990)

An EPR center labeled Si-*L*6 is reported which is identified as arising from the singly ionized acceptor state of isolated interstitial carbon (C_i^-) in electron-irradiated crystalline silicon. Correlated deep-level capacitance transient spectroscopy measurements locate the acceptor level at $E_c-0.10$ eV. The core structure of the defect is a $\langle 100\rangle$ C—Si interstitialcy similar to that previously proposed for C_i^+. The spin wave function is substantially more diffuse, however.

I. INTRODUCTION

Carbon is a common substitutional impurity (C_s) in crystalline silicon. Its concentration is typically in the range $10^{16}-10^{17}$ cm^{-3} in both floating-zone- (FZ) and Czochralski-grown materials. When silicon undergoes radiation damage, mobile Si interstitials produced in the primary damage event[1] can in turn displace C_s atoms to produce carbon interstitials (C_i).[2,3] The first detection of C_i was made using infrared absorption[2] via localized vibrational modes at 930 and 921 cm^{-1}. The C_i defect was subsequently identified in *p*-type material through electron paramagnetic resonance (EPR) (Ref. 3) and, later, its corresponding donor level was identified by deep-level capacitance transient spectroscopy (DLTS).[4] More recently, an electronic absorption band at 856 meV has also been identified as arising from the C_i defect.[5,6]

The EPR identification of C_i^+ was made by Watkins and Brower in *p*-type material from the so-called Si-*G*12 spectrum.[3] With a specially carbon-enriched (60% ^{13}C–40% ^{12}C) sample, hyperfine satellites reflecting the ^{13}C ($I=\frac{1}{2}$) isotopic abundance revealed unambiguously that a single carbon atom was incorporated in the defect. The model deduced for the Si-*G*12 center was a $\langle 100\rangle$ C—Si interstitialcy centered on a single substitutional site, consistent with the observed C_{2v} point-group symmetry and ^{13}C hyperfine interactions. Uniaxial stress and recovery from the preferential alignment due to the stress supported the microscopic model.[3]

In DLTS studies it was found that a peak at $E_v+0.28$ eV (Refs. 4 and 7) in room-temperature electron-irradiated *p*-type silicon had a very similar formation and annealing behavior as the Si-*G*12 center in EPR (Ref. 3) and the 930- and 921-cm^{-1} vibrational modes in ir studies.[2] The introduction rate of the defect was found to be independent of the acceptor doping impurity or growth technique. The level was therefore assigned to the single donor level (0/+) of the isolated carbon interstitial, known to exist from the EPR observation of C_i^+. In *n*-type material, on the other hand, a similarly behaved DLTS peak at $\sim E_c-0.10$ eV was also observed.[4] By injecting minority carriers into the *n*-type diodes, the $E_v+0.28$ eV peak could also be monitored in the same diodes as the $E_c-0.10$ eV peak and it was found that the two peaks came in and annealed out together.[4] On the basis of this, the $E_c-0.10$ eV peak was assigned as arising from a single-acceptor level (−/0) of C_i.[4,8] At the time, however, no EPR spectrum had been reported that could be related to C_i^-, which should be paramagnetic. Microscopic confirmation of this assignment was therefore missing.

In this paper we present EPR experimental results, in combination with DLTS studies, which for the first time establish that the $E_c-0.10$ eV level is indeed the single-acceptor level of interstitial carbon. We report a new EPR spectrum, Si-*L*6,[9] which we identify as arising from negatively charged C_i^-. External uniaxial stress alignment and recovery reveal that the core structure of Si-*L*6 is similar to that of the Si-*G*12 center for C_i^+. In a specially carbon-enriched (60% ^{13}C–40% ^{12}C) sample, no resolvable ^{13}C hyperfine could be resolved in the Si-*L*6 spectrum. Weak but partially resolved ^{13}C hyperfine interactions, however, are observed in one of the direct products of the Si-*L*6 center anneal at 300–350 K. This product, Si-*G*17,[1] is the subject of the following paper, where it is established[10-12] to arise from the stable configuration of a bistable interstitial-carbon–substitutional-carbon pair in its negative charge state $(C_iC_s)^-$.[10-12] This serves to confirm the C_i^- identification of the Si-*L*6 center. The weak ^{13}C hyperfine interaction for C_i^- in its isolated and paired configuration is argued to be consistent with a simple molecular orbital model for the center.

II. EXPERIMENTAL PROCEDURE

The EPR experiments were performed on a 14-GHz balanced bolometer spectrometer which could be tuned to either absorption or dispersion. The samples were placed in the center of a TE_{011} microwave cavity located in a Janis varitemp cryostat and uniaxial stress was supplied via a stainless steel rod from an air piston outside the cryostat. The DLTS spectrometer was a home-made version consisting of a 10-MHz capacitance bridge with a double boxcar analyzer.

All samples were floating-zone-grown materials which had varying carbon and donor concentrations, as shown in Table I. The carbon (C_s) concentration [C] was deter-

TABLE I. Wafers and bulk samples used in this study. All materials were FZ grown with oxygen concentration below ir detection ([O] ≤ 2×10^{16} cm^{-3}).

Wafers	Bulk	Dopant concentration (cm^{-3})	[C] (cm^{-3})
n type			
No. 1	No.1 ("F3-114")	$n=[\mathrm{P}]\sim6\times10^{15}$	2.4×10^{16}
No. 2	No. 2 ("A127-27A")	$n=[\mathrm{P}]\sim1.2\times10^{15}$	1×10^{17}
No. 3	No. 3 ("A231-9A")	$n=[\mathrm{P}]\sim9\times10^{15}$	$\le10^{16}$
	No. 4 ["SL-210 (NTD)"]	$n=[\mathrm{P}]\sim3\times10^{15}$ $p=[\mathrm{B}]\sim1\times10^{15}$	1×10^{17} (^{13}C 60%)
p type			
No. 5	No. 5 ("A623-16B")	$p=[\mathrm{B}]\sim2.4\times10^{15}$	
	No. 6 ("SL-210")	$p=[\mathrm{B}]\sim1\times10^{15}$	1×10^{17} (^{13}C 60%)

mined by ir absorption measurements of its local mode at 607 cm^{-1} at room temperature[13,14] with the limit of detection $\sim10^{16}$ cm^{-3}. The interstitial oxygen concentration [O] was estimated from the intensity of its ir absorption band at 9 μm at room temperature.[14,15] For all of the samples the oxygen concentration was determined to be less than 2×10^{16} cm^{-3}, the limit of detection. The samples for DLTS studies were either Schottky-barrier diodes or *p*-*n* junctions formed by ion implantation to avoid additional oxygen incorporation into the junction. (Details of the diode fabrication are described in the following paper.[12]) The EPR samples were cut from the appropriate boule in the form of a rectangular parallelopiped with a ⟨110⟩ axis parallel to the long dimension (2.5 mm×2.5 mm×15–20 mm). The diode wafers and EPR samples were cut from adjacent regions of each boule.

A specially ^{13}C-enriched sample (SL-210, [B]$\sim10^{15}$ cm^{-3}) was obtained from K. L. Brower. Some of the SL-210 material was converted to *n* type by neutron-transmutation doping[16] by J. Farmer at the University of Missouri–Columbia. The final net donor concentration was $\sim2\times10^{15}$ cm^{-3}.

The irradiations were performed at room temperature with ~2.5-MeV electrons from a 3-MeV van de Graaff accelerator. The samples were mounted on an air-cooled (or water-cooled, for the EPR samples) aluminum block with a low beam current (≤2 μA/cm^2) to avoid a sample temperature rise during the irradiation.

III. RESULTS

A. DLTS studies

The $E_c-0.10$ eV level was observed immediately after room-temperature irradiation in all samples except sample No. 3 ([C] ≤ 10^{16} cm^{-3}). Its production rate was found to correlate directly with the [C] concentration.[17] When it anneals at 300–350 K, two new defects with DLTS peaks at $E_c-0.17$ eV and $E_c-0.44$ eV were observed to grow in in 1:1 correspondence. The $E_c-0.17$ eV defect, accidentally at the same position as the O-*V* pair,[18] has been found to be bistable[17,19–23] and evidence has been presented that its arises from a carbon interstitial-carbon substitutional $(\mathrm{C}_i\mathrm{C}_s)^-$ pair.[17,22,23] This will be confirmed in the following paper.[12] The defect at $E_c-0.44$ eV, in this case accidentally again at the same position as the P-*V* pair,[24] has been found to display four other metastable configurations forming a remarkable five-level metastable defect.[17,22,23,25,26] It has been tentatively identified as a carbon interstitial-phosphorus substitutional $(\mathrm{C}_i\mathrm{P}_s)$ pair.[17,22,23] The $E_c-0.10$ eV level appears therefore to be the precusor of two carbon interstitial-related pair defects.

The time constant for isochronal annealing of the $E_c-0.10$ eV level in the temperature region 300–350 K is plotted in Fig. 1 with different biases applied during the anneal (sample No. 1). There is a small (a factor of 2.5) increase in the annealing rate under zero bias but essentially the same activation energy (~0.73 eV). This is as expected because at the annealing temperature (300–350 K) the Fermi level in this lightly irradiated sample is estimated to be at $\sim E_c-0.20$ eV.[27] Most of the $E_c-0.10$

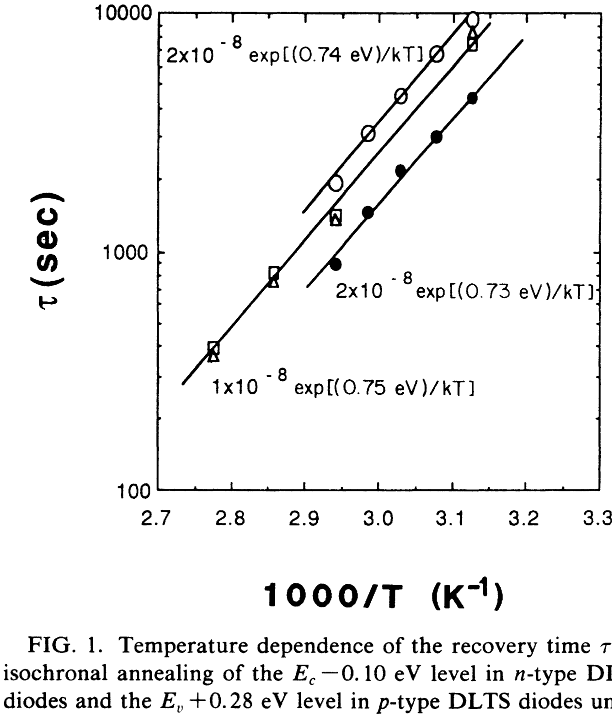

FIG. 1. Temperature dependence of the recovery time τ for isochronal annealing of the $E_c-0.10$ eV level in *n*-type DLTS diodes and the $E_v+0.28$ eV level in *p*-type DLTS diodes under different bias conditions: Zero bias (●, $E_c-0.10$ eV; □, $E_v+0.28$ eV); reverse bias (○, $E_c-0.10$ eV; △, $E_v+0.28$ eV).

eV centers were therefore in the same charge state under both bias conditions. The ~0.73 eV activation energy, therefore, should reflect the property of the uncharged defect. The 10^8 preexponential factor of the annealing kinetics strongly suggests long-range migration of the defect. It is fully consistent with a model for which the defect starts to migrate at 300–350 K and pairs off with another defect after ~10^5 jumps as an entity.[25]

The annealing kinetics of $C_i{}^+$ in the *p*-type sample No. 5 were also studied by monitoring the $E_v+0.28$ eV level. The results are also plotted in Fig. 1. The annealing rates and activation energies are very close to those in the *n*-type sample, and in this case no effect of bias was observed. The donor level for $C_i{}^+$ is 0.28 eV above the valence band and a large fraction of the defects should be positively charged under zero bias even at 300-350 K.[27] The results therefore suggest that the activation energy of 0.72–0.75 eV is the migration energy of C_i, which is independent of its charge state, at least for $C_i{}^+$ and $C_i{}^0$.

B. EPR studies

A new EPR spectrum was detected in the *n*-type samples immediately following room-temperature irradiation. The spectrum is labeled Si-*L*6, and is shown in Fig. 2(a).[9] It was taken at $T\sim30$ K with $\mathbf{B}\|\langle 100\rangle$, monitoring dispersion in the adiabatic fast passage case.[28] The appropriate spin Hamiltonian is

$$\mathcal{H}=\mu_B\mathbf{B}\cdot\underline{g}\cdot\mathbf{S} \tag{1}$$

with $S=\frac{1}{2}$. The angular dependence and spin-Hamiltonian parameters are given in Fig. 2 with the principal axes of the defect defined in Fig. 3. The spectrum has C_{2v} symmetry, similar to Si-*G*12 ($C_i{}^+$).[3] No resolved satellites associated with hyperfine interaction with a single ^{29}Si atom were found up to ±0.08 T indicating that the center is not a dangling-bond vacancy-type center.[1] In the *n*-type ^{13}C-enriched (60% ^{13}C) sample No. 4, no evidence of resolved ^{13}C hyperfine interaction could be detected which suggests that if carbon is involved in the center, the unpaired electron is only very weakly localized on the carbon atom.

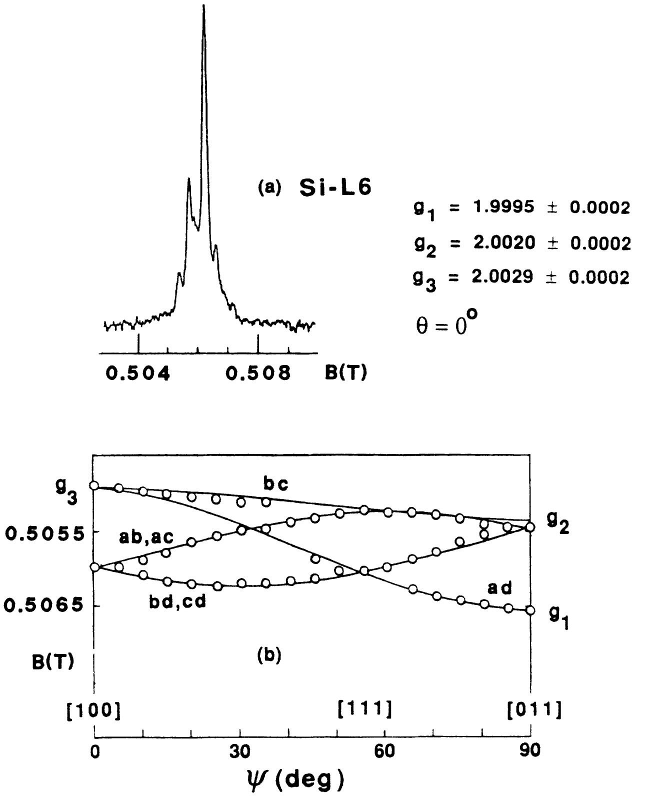

FIG. 2. (a) Si-*L*6 spectrum at $\upsilon=14.265$ GHz, $\mathbf{B}\|[100]$, $T\sim30$ K. The principal *g* values are shown for the defect coordinate system as defined in Fig. 3. (b) Angular dependence of the Si-*L*6 spectrum, with **B** in the $(0\bar{1}1)$ plane.

The Si-*L*6 spectrum was only detected in the samples for which [C] $\geq 10^{16}$ cm^{-3}, the same samples in which the $E_c-0.10$ eV precursor level was detected.[9] Its relative intensity among the various *n*-type samples of Table I, like the $E_c-0.10$ eV level, also appears proportional to [C] in the sample. The annealing behavior of the Si-*L*6 center is also very similar to the $E_c-0.10$ eV level, the spectrum disappearing in ~30 min at 350 K. Accompanying its disappearance, another EPR spectrum, previously reported and labeled Si-*G*17,[1,9] grows in. In the following paper (Ref. 12), we will establish that this new center arises from the negatively charged $(C_iC_s)^-$ pair.

To further correlate the Si-L6 EPR center with the $E_c-0.10$ eV level, we can make an approximate estimate of the Si-*L*6 defect-level position directly in the EPR experiment. Figure 4 is a plot of the EPR signal intensities versus irradiation dose. Initially, the Fermi level is locked on the phosphorus donors since few phosphorus atoms are ionized at the measuring temperature (~30 K). By increasing the radiation dose, more deep-level defects are created, which serve to remove electrons from the phosphorus donors. The phosphorus resonance

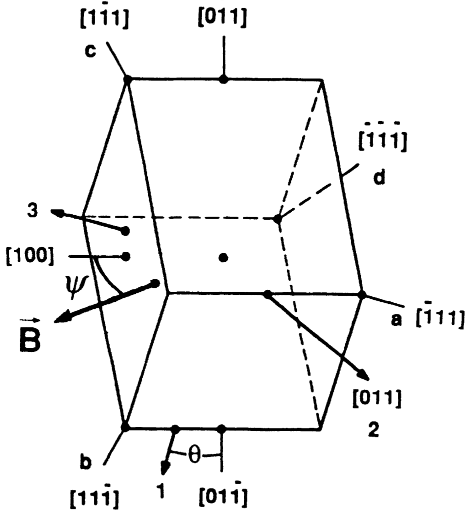

FIG. 3. Principal axes used for the spin-Hamiltonian parameters of the EPR spectra.

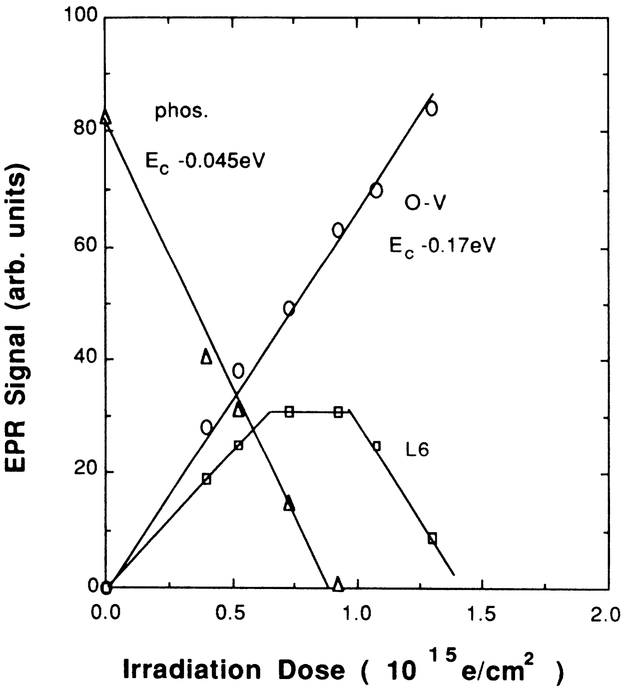

FIG. 4. EPR signal intensities as a function of electron irradiation dose for an n-type sample (sample No. 2). The results indicate that the energy-level position (E_t) of the Si-$L6$ center is $E_c-0.045$ eV $<E_t<E_c-0.17$ eV.

therefore decreases while the deeper-level signals increase [in this particular sample, a small amount of oxygen is present so we have both Si-$L6$ and O-V pair (A-center) EPR signals[18]]. When all the electrons are removed from the phosphorus, the Fermi level moves down to the next defect level, in this case the Si-$L6$ center. The Si-$L6$ signal therefore begins to decrease as electrons are removed from it by the continued production of deeper defects, while the A-center signal continues to increase. This demonstrates that the energy-level position of the Si-$L6$ center is deeper than the phosphorus donor (~ 0.045 eV below the conduction band[27,29]) but shallower than the O-V pair which has a level at $E_c-0.17$ eV.[30] This is fully consistent with the DLTS measurement of the $E_c-0.10$ eV level.

We have further studied the Si-$L6$ spectrum under uniaxial stress. The change in energy of a defect in the resulting strain, can be written

$$E=\mathrm{Tr}(\underline{B}\cdot\underline{\varepsilon}) , \tag{2}$$

where $\underline{B}$ is the "piezospectroscopic" tensor characteristic of the defect[31,32] and $\underline{\varepsilon}$ is the strain tensor. If the temperature is sufficiently high, the defects are free to reorient themselves amongst the various equivalent orientations and an applied stress will produce a preferential alignment. This alignment can then be "frozen-in" by cooling to low temperature with the stress on. In EPR, therefore, the relative populations in the different orientations can be determined directly from the relative intensities of the corresponding lines.

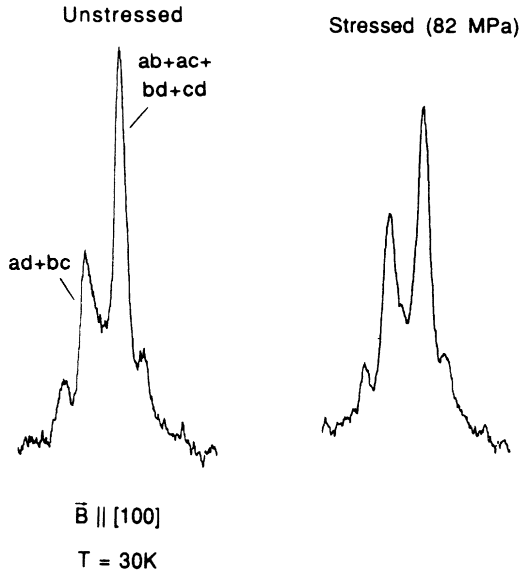

FIG. 5. The Si-$L6$ spectrum shown before and after ~ 270 K compressional stress $\sigma \| [0\bar{1}1]$; $\mathbf{B} \| [100]$.

The labeling scheme shown in Fig. 2(b) arises as follows: The four $\langle 111 \rangle$ axes are labeled a, b, c, and d. This is illustrated in Fig. 3. We label a defect by two letters. The first letter specifies the $\langle 111 \rangle$ axis closest to the g_3 axis of a defect orientation and the second specifies the $\langle 111 \rangle$ axis closest to the g_1 axis. In Fig. 3, the specific defect axes illustrated correspond to defect cb. For a C_{2v} center such as Si-$L6$, defect (ij) and (ji) are identical and in Fig. 2(b) only one of these labels is indicated.

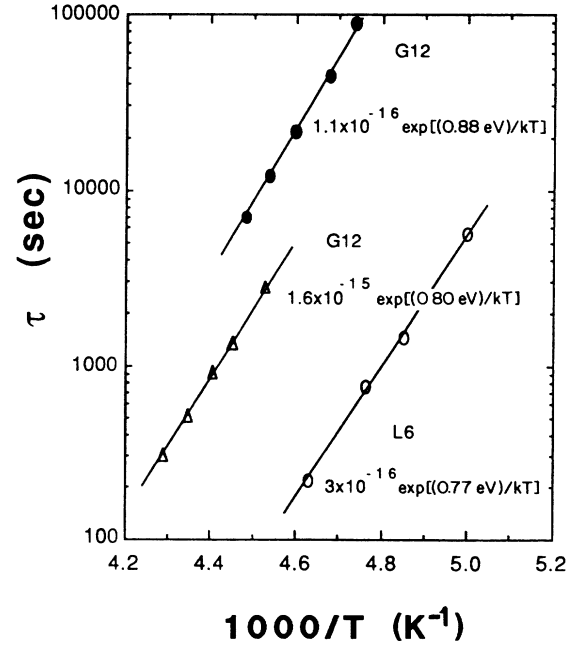

FIG. 6. Temperature dependence of the characteristic time constant τ for recovery of the alignment for the Si-$L6$ and Si-$G12$ centers: ○, Si-$L6$; △, Si-$G12$, our results; ●, Si-$G12$, Ref. 3.

TABLE II. Components of the traceless elastic coupling tensor, $\underline{B}$, for the Si-$L6$ and Si-$G12$ centers (the defect principal axes are given in Fig. 3).

Si-$L6$ (eV)	Si-$G12^{a}$ (eV)
$B_1=7.4$	$B_1=7.3$
$B_2=-0.2$	$B_2=0.3$
$B_3=-7.2$	$B_3=-7.6$

[a] Reference 3.

The Si-$L6$ center shows a preferential alignment when external uniaxial stress (~ 82 MPa) is applied at $T \geq 270$ K and the sample is cooled with the stress on to the EPR measuring temperature (~ 30 K). The results are shown in Fig. 5 for stress $\sigma \parallel [0\bar{1}1]$ and $\mathbf{B} \parallel [100]$ where the individual lines are labeled according to the convention. By measuring the intensities of these lines before and after the stress and combining with measurements for $\mathbf{B} \parallel [011]$ to give the relative amplitude changes of *ad* and *bc*, we compute the principal values of the traceless component of $\underline{B}$, assuming a Boltzmann distribution between the differently oriented defects at the quench-in temperature (~ 220 K, estimated from the recovery kinetics, Fig. 6, which are described in the next paragraph). The results are given in Table II along with those for the C_i^+ Si-$G12$ center for comparison.[3] The two sets of data are remarkably similar, which provides strong evidence that the two spectra actually arise from the same center.

Recovery from the alignment for both the Si-$L6$ and Si-$G12$ centers was studied by a series of isothermal anneals. The results are shown in Fig. 6, together with the previous data reported for Si-$G12$.[3] The reorientation energy barrier for Si-$L6$ is determined to be ~ 0.77 eV, very close to what we determine for Si-$G12$, ~ 0.80 eV. They are not identical, however, but we do not expect the properties of two different charge states of a single defect to be the same. (Note that our measured values for $G12$ are a factor of ~ 3 faster than those previously reported[3] and with a lower activation energy, 0.80 versus 0.88 eV. Whether this represents inaccuracies in temperature determinations between ours and the earlier measurements or whether it represents a real sample dependence is an important question but not relevant to our conclusions here as regards the similarity between Si-$L6$ and Si-$G12$.)

IV. MODEL AND CONCLUSIONS

We conclude that the Si-$L6$ EPR spectrum arises from the negative charge state of isolated interstitial carbon. This provides the first microscopic confirmation that an acceptor state of C_i does indeed exist in the band gap, and from correlative DLTS studies, we conclude that the acceptor level is at $E_c - 0.10$ eV, as previously proposed.[4,8]

The microscopic model we propose for the C_i^- state is shown in Fig. 7. The atomic structure is essentially the same as that proposed for C_i^+ (Si-$G12$).[3] The $\langle 100 \rangle$-oriented C—Si interstitialcy core structure remains, consistent with the C_{2v} symmetry of the EPR spectrum and the uniaxial stress and recovery results which are almost identical for the two.

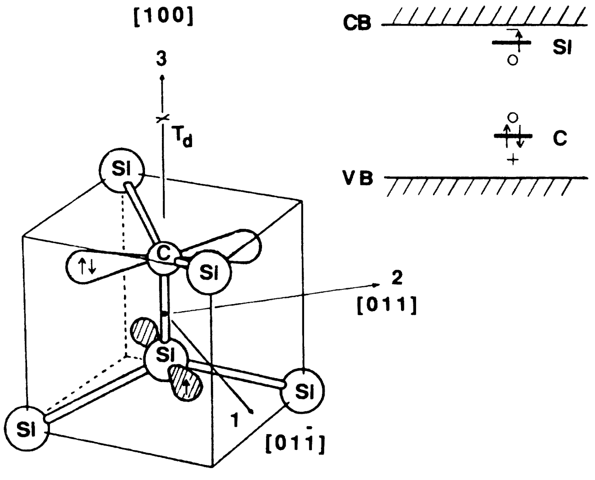

FIG. 7. A model for the Si-$L6$ center.

In the figure we show also a simple molecular orbital model for the defect. In the case of C_i^+, the unpaired electron is localized in the nonbonding *p* orbital of the carbon atom due to its larger electronegativity than silicon. The ^{13}C hyperfine interaction is therefore strong, as observed.[3] However, in adding two more electrons to form C_i^-, the unpaired electron is now in the nonbonding *p* orbital of the silicon atom, explaining the failure to detect the ^{13}C interaction in Si-$L6$. This molecular orbital picture agrees well with recent preliminary theoretical calculations for the acceptor state of the isolated interstitial carbon.[33] However, failure to detect a single ^{29}Si hyperfine interaction from the C_i^- state suggests that the unpaired electron is actually not strongly localized on this single interstitial silicon atom, but is rather more diffuse. A possible explanation for this has also been cited in these recent calculations, where the existence of a different more extended available state of comparable energy was also noted.[33] Future experiments with electron-nuclear double resonance would be desirable to illustrate these points, as well as to provide direct confirmation of the ^{13}C involvement.

As noted by previous workers[3] and discussed briefly earlier, we might expect the same activation energy for reorientation and annealing if the reorientation and single diffusional jump mechanisms are the same. Recent annealing results by Tipping and Newman[34] for the 856-meV optical band identified with C_i gave an activation energy of 0.87 eV and they noted the close similarity to the 0.88-eV reorientation barrier reported earlier by Watkins and Brower for Si-$G12$.[3] Our results here indicate uniformly lower activation energies for both reorientation (0.77–0.80 eV) and annealing (0.73 eV), but again similar to each other. The reason for the discrepancy between these two sets of results is not clear. Besides the trivial explanation of possible inaccuracies in temperature determinations, we note that these other studies involved considerably more heavily irradiated materials. Just how this would affect the annealing or reorientation kinetics is not clear, however, in view of the fact that we have established that Fermi-level effects alone appear not to be important. Further experiments would be desirable to clarify this question.

ACKNOWLEDGMENTS

This work was supported by the United States Office of Naval Research Contract No. N00014-84-K-0025.

---

[*] Present address: Department of Physics and New York State Institute on Superconductivity, State University of New York at Buffalo, Amherst, NY 14260.

[1] G. D. Watkins, in *Radiation Damage in Semiconductors,* edited by P. Baruch (Dunod, Paris, 1964), p. 97.

[2] A. R. Bean and R. C. Newman, Solid State Commun. **8**, 175 (1970).

[3] G. D. Watkins and K. L. Brower, Phys. Rev. Lett. **36**, 1329 (1976).

[4] L. C. Kimerling, P. Blood, and W. M. Gibson, in *Defects and Radiation Effects in Semiconductors, 1978,* IOP Conf. Proc. Ser. No. 46, edited by J. H. Albany (IOP, London, 1979), p. 273.

[5] R. Woolley, E. C. Lightowlers, A. K. Tipping, M. Claybourn, and R. C. Newman, in *Proceedings of the 14th International Conference on Defects in Semiconductors,* edited by H. J. von Bardeleben (Trans Tech, Aedermannsdorf, Switz., 1989); Mater. Sci. Forum **10-12**, 929 (1986).

[6] K. Thonke, A. Teschner, and R. Sauer, Solid State Commun. **61**, 24 (1987).

[7] Y. H. Lee, L. J. Cheng, J. D. Gerson, P. M. Mooney, and J. W. Corbett, Solid State Commun. **21**, 109 (1977).

[8] R. D. Harris and G. D. Watkins, in *The 13th International Conference on Defects in Semiconductors,* edited by L. C. Kimerling and J. M. Parsey, Jr. (AIME, New York, 1985), p. 799.

[9] L. W. Song and G. D. Watkins, Bull. Am. Phys. Soc. **32**, 403 (1987).

[10] L. W. Song, X. D. Zhan, B. W. Benson, and G. D. Watkins, in *Defects in Electronic Materials,* Vol. 104 of *Materials Research Society Symposia Proceedings,* edited by M. Stavola, S. J. Pearton, and G. Davies (MRS, Pittsburgh, 1988), p. 79.

[11] L. W. Song, X. D. Zhan, B. W. Benson, and G. D. Watkins, Phys. Rev. Lett. **60**, 460 (1988).

[12] L. W. Song, X. D. Zhan, B. W. Benson, and G. D. Watkins, following paper, Phys. Rev. B **42**, 5765 (1990).

[13] R. C. Newman and J. B. Willis, J. Phys. Chem. Solids **26**, 373 (1965).

[14] *Annual Book of ASTM Standards* (ASTM, Philadelphia, 1988), Vol. 10.05.

[15] W. Kaiser, P. H. Keck, and C. F. Lange, Phys. Rev. **101**, 1264 (1956).

[16] J. M. Meese, *Neutron Transmutation Doping in Semiconductors* (Plenum, New York, 1979).

[17] L. W. Song, B. W. Benson, and G. D. Watkins, Appl. Phys. Lett. **51**, 1155 (1987).

[18] G. D. Watkins and J. W. Corbett, Phys. Rev. **101**, 1001 (1961).

[19] G. E. Jellison, Jr., J. Appl. Phys. **53**, 5715 (1982).

[20] J. L. Benton and M. Levinson, in *Defects iin Semiconductors II,* edited by S. Mahajan and J. W. Corbett (North-Holland, New York, 1983), p. 95.

[21] A. Chantre and D. Bois, Phys. Rev. B **31**, 7979 (1985).

[22] A. Chantre and L. C. Kimerling, Appl. Phys. Lett. **48**, 1000 (1986).

[23] M. T. Asom, J. L. Benton, R. Sauer, and L. C. Kimerling, Appl. Phys. Lett. **51**, 256 (1987).

[24] G. D. Watkins and J. W. Corbett, Phys. Rev. **134**, A1359 (1964).

[25] L. W. Song, B. W. Benson, and G. D. Watkins, Phys. Rev. B **33**, 1452 (1986).

[26] E. Gurer and B. W. Benson, Bull. Am. Phys. Soc. **34**, 834 (1989).

[27] S. M. Sze, *Physics of Semiconductor Devices,* 1st ed. (Wiley, New York, 1981).

[28] A. M. Portis, Sarah Mellon Scaife Radiation Laboratory, Technical Note No. 1, 1955 (unpublished).

[29] A. G. Milnes, *Deep Impurities in Semiconductors* (Wiley, New York, 1973).

[30] L. C. Kimerling, in *Radiation Effects in Semiconductors,* IOP Conf. Proc. Ser. No. 31, edited by N. B. Urli and J. W. Corbett (IOP, London, 1977), p. 221.

[31] A. A. Kaplyanskii, Opt. Spectrosc. **16**, 329 (1964).

[32] Y. H. Lee and J. W. Corbett, Phys. Rev. B **9**, 4351 (1974).

[33] M. Besson, G. G. Deleo, and W. B. Fowler, Bull. Am. Phys. Soc. **32**, 404 (1987).

[34] A. K. Tipping and R. C. Newman, Semicond. Sci. Technol. **2**, 315 (1987).